

Hadron physics with KLOE-2

Eryk Czerwiński¹ on behalf of KLOE-2 collaboration²

Laboratori Nazionali di Frascati – INFN, Via E. Fermi 40, I-00044 Frascati (Rome) Italy

Abstract

In the upcoming month the KLOE-2 data taking campaign will start at the upgraded DAΦNE ϕ -factory of INFN Laboratori Nazionali di Frascati. The main goal is to collect an integrated luminosity of about 20 fb^{-1} in 3-4 years in order to refine and extend the KLOE program on both kaon physics and hadron spectroscopy. Here the expected improvements on the results of hadron spectroscopy are presented and briefly discussed.

Keywords: e^+e^- collisions, meson transition form factors, π pair production, σ meson
2010 MSC: 81-05, 81-06

1. KLOE-2 detector at upgraded DAΦNE collider

The KLOE detector setup consists of a large drift chamber (radius from 0.25 to 2.0 m and 3.3 m length) surrounded by an electromagnetic calorimeter. Both are immersed in 0.52 T axial field of superconducting solenoid [1]. From 2000 to 2006 the KLOE experiment has collected 2.5 fb^{-1} at the peak of the ϕ meson resonance at the e^+e^- collider DAΦNE in Frascati plus additional 250 pb^{-1} of off-peak data.

A new beam crossing scheme is operating at DAΦNE allowing to reduce beam size and increase luminosity (to reach a peak of about $5 \times 10^{32} \text{ cm}^{-2} \text{ s}^{-1}$, a factor of 3 larger than the previously obtained). At the moment, the detector is being upgraded with small angle tagging devices, to detect both low (Low Energy Tagger - LET) and high (High Energy Tagger - HET) energy e^+e^- originated from $e^+e^- \rightarrow e^+e^-X$ reactions. It is planned to collect around 5 fb^{-1} within one year with this setup.

In a subsequent step a light-material Inner Tracker (IT) will be installed in the region between the beam pipe and the drift chamber to improve charged vertex reconstruction and to increase the acceptance for low transversal momentum tracks [2]. Crystal calorimeters (CCALT) will cover the low θ region to increase acceptance for very forward electrons and photons down to 8° . A new tile calorimeter (QCALT) will be used for the detection of photons coming from K_L decays in the drift chamber. Implementation of the second step is planned for late 2011. Further modifications of the DAΦNE collider, presently under discussion, would allow energies up to 2.5 GeV (\sqrt{s}) to be reached without loss of luminosity. Since the KLOE-2 detector is perfectly suited for data taking also at energies away from the ϕ meson mass, a proposal to perform precision measurements of (multi)hadronic and $\gamma\gamma$ cross sections has also been put forward [3]. The detailed description of the KLOE-2 physics program can be found in Ref. [4].

¹*Email address:* eryk.czerwinski@lnf.infn.it

²KLOE-2 collaboration: F. Archilli, D. Babusci, D. Badoni, G. Bencivenni, C. Bini, C. Bloise, V. Bocci, F. Bossi, P. Branchini, A. Budano, S. A. Bulychjev, P. Campana, G. Capon, F. Ceradini, P. Ciambrone, E. Czerwiński, E. Dané, E. De Lucia, G. De Robertis, A. De Santis, G. De Zorzi, A. Di Domenico, C. Di Donato, B. Di Micco, D. Domenici, O. Erriquez, G. Felici, S. Fiore, P. Franzini, P. Gauzzi, S. Giovannella, F. Gonnella, E. Graziani, F. Happacher, B. Höistad, E. Iarocci, M. Jacewicz, T. Johansson, V. Kulikov, A. Kupsc, J. Lee-Franzini, F. Loddo, M. Martemianov, M. Martini, M. Matsyuk, R. Messi, S. Miscetti, D. Moricciani, G. Morello, P. Moskal, F. Nguyen, A. Passeri, V. Patera, A. Ranieri, P. Santangelo, I. Sarra, M. Schioppa, B. Sciascia, A. Sciubba, M. Silarski, S. Stucci, C. Taccini, L. Tortora, G. Venanzoni, R. Versaci, W. Wiślicki, M. Wolke, J. Zdebik

2. $\gamma\gamma$ physics

The term $\gamma\gamma$ physics (or *two photon physics*) stands for the study of the reaction:

$$e^+e^- \rightarrow e^+e^- \gamma^* \gamma^* \rightarrow e^+e^- X, \quad (1)$$

where X is an arbitrary hadronic state with quantum numbers $J^{PC} = 0^{\pm\pm}, 2^{\pm\pm} \dots$ and the two photons tend to be quasi-real [5]. If no cut is applied to the final-state leptons, the Weizsäcker-Williams approximation [6] can be used to understand the main qualitative features

of process (1). Then the event yield, N_{eeX} , can be evaluated according to:

$$N_{eeX} = L_{ee} \int \frac{dF}{dW_{\gamma\gamma}} \sigma_{\gamma\gamma \rightarrow X}(W_{\gamma\gamma}) dW_{\gamma\gamma}, \quad (2)$$

where $W_{\gamma\gamma}$ is the invariant mass of the two quasi-real photons, L_{ee} is the integrated luminosity, and $dF/dW_{\gamma\gamma}$ is the $\gamma\gamma$ flux function:

$$\frac{dF}{dW_{\gamma\gamma}} = \frac{1}{W_{\gamma\gamma}} \left(\frac{2\alpha}{\pi} \right)^2 \left(\ln \frac{E_b}{m_e} \right)^2 f(z), \quad (3)$$

where E_b is the beam energy and

$$f(z) = (z^2 + 2)^2 \ln \frac{1}{z} - (1 - z^2)(3 + z^2), \quad z = \frac{W_{\gamma\gamma}}{2E_b}. \quad (4)$$

Figure 1 shows examples of the $\gamma\gamma$ flux functions multiplied by an integrated luminosity $L_{ee} = 1 \text{ fb}^{-1}$, as a function of the $\gamma\gamma$ invariant mass for different center-of-mass energies; threshold openings of different hadronic states are indicated. Previous experiments measured the $\gamma\gamma$ cross section for pseudoscalar meson production in the range $7 < \sqrt{s} < 35 \text{ GeV}$. A low energy e^+e^- collider, such as DAΦNE, compensates the small cross section value with the high luminosity.

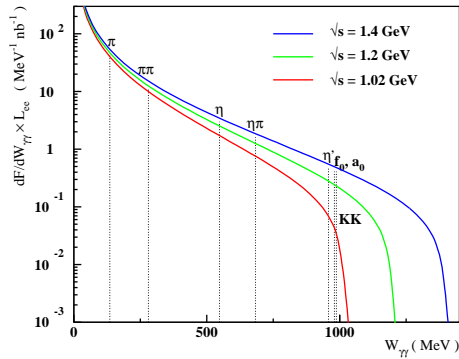


Figure 1: Differential $\gamma\gamma$ flux function as a function of the center-of-mass energy.

3. Meson transition form factors

The transition form factors $\mathcal{F}_{P\gamma\gamma^*}(m_P^2, q_1^2, q_2^2)$ at space-like momentum transfers can be measured with process (1). They are important to discriminate among different phenomenological models relevant for the hadronic light-by-light scattering contribution to the $g - 2$ of the muon [7].

The form factor at negative q^2 appears in the production cross section of π^0 , η and η' mesons in the reaction $e^+e^- \rightarrow e^+e^-P$. By detecting one electron at

large angle with respect to the beams, the form factor $\mathcal{F}_{P\gamma\gamma^*}(m_P^2, Q^2, 0)$ with one quasi-real and one virtual space-like photon ($Q^2 = -q^2$) can be measured for the on-shell pseudoscalar meson. For both π^0 and η mesons the region below 1 GeV^2 is still poorly known but can be covered by KLOE-2. Furthermore, by selecting events in which both e^+ and e^- are detected by the drift chamber (instead of the tagger devices) KLOE-2 can provide experimental information on form factors $\mathcal{F}_{P\gamma^*\gamma^*}(m_P^2, Q_1^2, Q_2^2)$, with two virtual photons.

4. $\gamma\gamma \rightarrow \pi\pi$

The two photon production of hadronic resonances is often advertised as one of the clearest ways of revealing their composition [8–18]. KLOE-2 with the study of $e^+e^- \rightarrow e^+e^-\pi\pi$ decays can improve the experimental precision in the following energy ranges contributing to the solution of the open questions on low-energy hadron physics:

- 280-450 MeV: The Mark II experiment [19] is the only one that has made a special measurement of the normalized cross-section for the $\pi^+\pi^-$ channel near threshold, however, their data have very large error-bars;
- 450-850 MeV: Measure $\pi\pi$ production in this region in both charge modes for our understanding of strong QCD coupling and the nature of the vacuum [20];
- 850-1100 MeV: Accurate measurement of the $\pi^+\pi^-$ and $\pi^0\pi^0$ cross-sections (integrated and differential).

The $e^+e^- \rightarrow e^+e^-\pi\pi$ process is a clean electromagnetic probe to investigate the nature of the σ meson through the analysis of the $\pi\pi$ invariant mass which is expected to be plainly affected by the presence of this scalar meson. A precision measurement of the cross-section of $\gamma\gamma \rightarrow \pi^+\pi^-$ and $\gamma\gamma \rightarrow \pi^0\pi^0$ would also complete the information from previous experiments allowing the determination of the $\gamma\gamma$ couplings of the scalar mesons.

4.1. $\gamma\gamma \rightarrow \pi^0\pi^0$

The interest in this process is given by the $\sigma \rightarrow \pi\pi$ contribution [21]. The determination of the $\sigma\gamma\gamma$ coupling can be compared with that of pseudoscalars or other scalar states to clarify their quark structure. From Figure 2, an excess of about 4000 events with respect to the expected background is evident at low 4 photons invariant mass ($M_{4\gamma}$) values, consistent in shape with

expectations [22] from $e^+e^- \rightarrow e^+e^-\pi^0\pi^0$ events. The precise yield estimate depends on assumptions for the background processes. Systematic study of the differential cross section and understanding of the $\sigma \rightarrow \pi\pi$ contribution are in progress.

The studies point out that KLOE-2 with an integrated luminosity at the ϕ peak of $L = 5 \text{ fb}^{-1}$ can measure the $\gamma\gamma \rightarrow \pi^0\pi^0$ cross-section with the same energy binning obtained from Crystal Ball [23], reducing the statistical uncertainty in each bin to 2%.

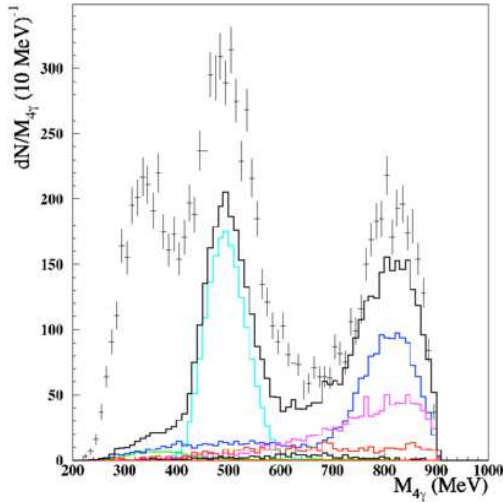


Figure 2: Preliminary spectrum of the 4 photons invariant mass obtained with KLOE detector, compared with sum of the expected backgrounds. Peak of the $K_S \rightarrow \pi^0\pi^0$ decay and structures related to other processes with two π^0 are visible: $\omega(\rightarrow \pi^0\gamma)\pi^0$ and $f_0(980)(\rightarrow 2\pi^0)\gamma$. The cut on $M_{4\gamma} < 900 \text{ MeV}$ is explained by the requirement on the total energy in the calorimeter.

5. $\eta \rightarrow \pi^0\gamma\gamma$

Using the KLOE preliminary result on the branching fraction and the analysis efficiency obtained of $\sim 5\%$, 1300 $\eta \rightarrow \pi^0\gamma\gamma$ events are expected from the first year of data-taking at KLOE-2, thus allowing an accuracy of 3% to be reached on the $\text{BR}(\eta \rightarrow \pi^0\gamma\gamma)$. Moreover, KLOE-2 can provide the $m_{\gamma\gamma}$ distribution with sufficient precision to solve the ambiguity connected to the sign of the interference between VMD and scalar terms as shown in Figure 3.

6. $\eta' \rightarrow \eta\pi\pi$

In the $\eta' \rightarrow \eta\pi^+\pi^-$ and $\eta' \rightarrow \eta\pi^0\pi^0$, the $\pi\pi$ system is produced mostly with scalar quantum numbers. Indeed, the available kinetic energy of the $\pi^+\pi^-$

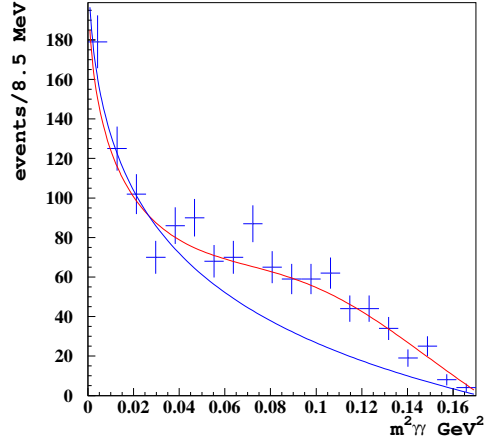


Figure 3: The $m_{\gamma\gamma}^2$ distribution in $\eta \rightarrow \pi^0\gamma\gamma$ decays expected at KLOE-2 for the VMD+ $a_0(980)$ model, with constructive and destructive interference term. Crosses are the simulated experimental data assuming 5% constant efficiency as a function of $m_{\gamma\gamma}^2$ and constructive interference.

pair is [0, 137] MeV, suppressing high angular momentum contribution. Furthermore, the exchange of vector mesons is forbidden by G-parity conservation. For these reasons, only scalar mesons can participate to the scattering amplitude. The decay can be mediated by the σ , $a_0(980)$ and $f_0(980)$ exchange and by a direct contact term due to the chiral anomaly [24]. The scalar contribution can be determined by fitting the Dalitz plot of the $\eta' \rightarrow \eta\pi\pi$ system. The golden channel for KLOE-2 is the decay chain $\eta' \rightarrow \eta\pi^+\pi^-$, with $\eta \rightarrow \gamma\gamma$. The signal can be easily identified from the η and η' invariant masses. Such final state was already studied at KLOE to measure the branching fraction of the $\phi \rightarrow \eta'\gamma$ decay [25]. The analysis efficiency was 22.8%, with 10% residual background contamination. With $\mathcal{O}(10) \text{ fb}^{-1}$, we expect 80,000 fully reconstructed events. In Figure 4 the $m_{\pi^+\pi^-}$ invariant mass distribution is shown with and without the σ contribution with the expected KLOE-2 statistics.

7. η/η' mixing

The η' meson, being almost a pure $\text{SU}(3)_{\text{Flavor}}$ singlet, is considered a good candidate to host a gluon condensate. KLOE has extracted the η' gluonium content and the η - η' mixing angle [26] according to the model of Ref. [27]. The η and η' wave functions can be decomposed in three terms: the u, d quark wave function $|q\bar{q}\rangle = \frac{1}{\sqrt{2}}(|u\bar{u}\rangle + |d\bar{d}\rangle)$, the $|s\bar{s}\rangle$ component and the gluonium $|GG\rangle$. The wave functions are written as: $|\eta'\rangle = \cos\psi_G \sin\psi_P |q\bar{q}\rangle + \cos\psi_G \cos\psi_P |s\bar{s}\rangle +$

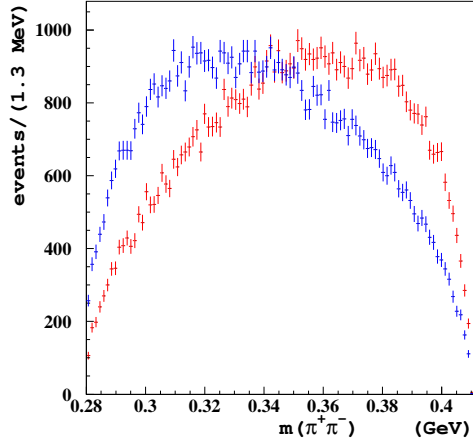


Figure 4: The $m_{\pi^+\pi^-}$ distribution in the $\eta' \rightarrow \eta\pi^+\pi^-$ decay with the σ meson (right-centered distribution) and without (left-centered distribution) contribution.

$\sin\psi_G |GG\rangle$ and $|\eta\rangle = \cos\psi_P |q\bar{q}\rangle - \sin\psi_P |s\bar{s}\rangle$ where ψ_P is the η - η' mixing angle and $Z_G^2 = \sin^2\psi_G$ is the gluonium fraction in the η' meson. The Z_G^2 parameter can be interpreted as the mixing with a pseudoscalar glueball.

With the KLOE-2 data-taking above the ϕ peak, e.g., at $\sqrt{s} \sim 1.2$ GeV, it will be possible to measure the η' decay width $\Gamma(\eta' \rightarrow \gamma\gamma)$ through the measurement of the reaction $\sigma(e^+e^- \rightarrow e^+e^-(\gamma^*\gamma^*) \rightarrow e^+e^-\eta')$. The measurement to 1% level of both the cross section and the $BR(\eta' \rightarrow \gamma\gamma)$ would bring the fractional error on the η' total width, $\Gamma_{\eta'} = \Gamma(\eta' \rightarrow \gamma\gamma)/BR(\eta' \rightarrow \gamma\gamma)$, to $\sim 1.4\%$. Figure 5 shows the 68% C.L. region in the ψ_P, Z_G^2 plane obtained with the improvements discussed in this section. The comparison of the top to bottom panels makes evident how the fit accuracy increases with the precision measurement of the η' total width.

References

- [1] M. Adinolfi *et al.*, Nucl. Phys. **A663** 1103 (2000).
- [2] F. Archilli *et al.*, arXiv:1002.2572 (2010).
- [3] D. Babusci *et al.*, LNF note 10/17(P), arXiv:1007.5219 (2010).
- [4] G. Amelino-Camelia *et al.*, Eur. Phys. J. **C68** 619 (2010).
- [5] C.N. Yang, Phys. Rev. **77** 242 (1950).
- [6] S.J. Brodsky, T. Kinoshita, H. Terazawa, Phys. Rev. **D4** 1532 (1971).
- [7] F. Jegerlehner, A. Nyffeler, Phys. Rept. **477** 1 (2009).
- [8] E. van Beveren, F. Kleefeld, G. Rupp, M.D. Scadron, Phys. Rev. **D79** 098501 (2009).
- [9] C. Hanhart, Y.S. Kalashnikova, A.E. Kudryavtsev, A.V. Nefediev, Phys. Rev. **D75** 074015 (2007).
- [10] T. Branz, T. Gutsche, V.E. Lyubovitskij, Phys. Rev. **D78** 114004 (2008).
- [11] M.K. Volkov, E.A. Kuraev, Y.M. Bystritskiy, 0904.2484 (2009).

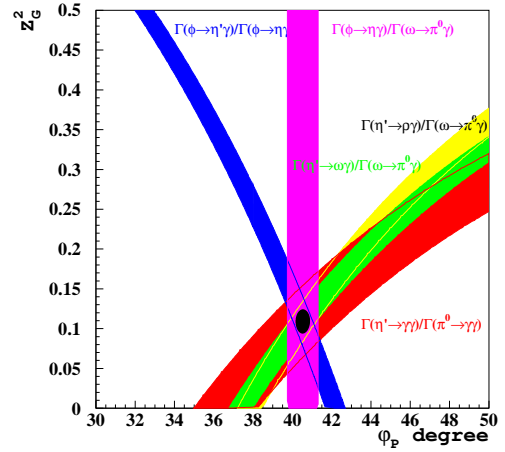
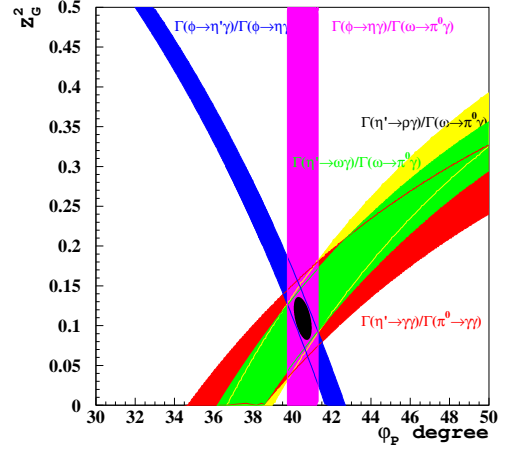


Figure 5: The 68% C.L. region in the ψ_P, Z_G^2 plane. Top: only the η' branching ratios are improved to 1% precision. Bottom: the η' total width is also lowered to 1.4%.

- [12] G. Mennessier, S. Narison, W. Ochs, Phys. Lett. **B665** 205 (2008).
- [13] N.N. Achasov, G.N. Shestakov, Phys. Rev. **D77** 074020 (2008).
- [14] F. Giacosa, AIP Conf. Proc. **1030** 153 (2008).
- [15] F. Giacosa, T. Gutsche, V.E. Lyubovitskij, Phys. Rev. **D77** 034007 (2008).
- [16] E. Klempt, A. Zaitsev, Phys. Rept. **454** 1 (2007).
- [17] M.R. Pennington, 0711.1435 (2007).
- [18] T. Barnes, Phys. Lett. **B165** 434 (1985).
- [19] J. Boyer *et al.*, Phys. Rev. **D42** 1350 (1990).
- [20] M.R. Pennington, Mod. Phys. Lett. **A22** 1439 (2007).
- [21] C. Amsler *et al.*, Phys. Lett. **B667** 1 (2008).
- [22] F. Nguyen, Chin. Phys. (HEP & NP) **C34** 1 (2010).
- [23] H. Marsiske *et al.*, Phys. Rev. **D41** 3324 (1990).
- [24] A.H. Fariborz, J. Schechter, Phys. Rev. **D60** 034002 (1999).
- [25] A. Aloisio *et al.*, Phys. Lett. **B541** 45 (2002).
- [26] F. Ambrosino *et al.*, JHEP **07** 105 (2009).
- [27] J.L. Rosner, Phys. Rev. **D27** 1101 (1983).